

## Fluctuations and Shear Modulus of a Classical Two-Dimensional Electron Solid: Experiment

F. Gallet, G. Deville, A. Valdès, and F. I. B. Williams

*Service de Physique du Solide et de Résonance Magnétique, Institut de Recherche Fondamentale, Centre d'Etudes Nucléaires de Saclay, 91191 Gif-sur-Yvette Cédex, France*

(Received 6 July 1981)

The shear modulus of two-dimensional electrons at the surface of liquid helium is deduced from measurements of the finite frequency of the  $k \rightarrow 0$  limit of the coupled electron-substrate transverse sound mode. Its behavior on the approach to melting is compatible with the Kosterlitz-Thouless model for two-dimensional melting.

PACS numbers: 64.70.Dr

It is now well established<sup>1-3</sup> that electrons on the surface of liquid helium undergo a phase transition to a spatially ordered state at low temperatures. This very simple and clean example of a two-dimensional smooth-substrate (translationally invariant) system provides an excellent testing ground for understanding two-dimensional melting. In the belief that one of the keys to this study lies in the behavior of the shear elastic modulus, we have designed an experiment to measure this in two ways: (i) by its effect on the electron thermal fluctuations which determine the helium surface deformation, and (ii) more directly by the velocity of transverse sound. It is the results of the first part (i) that are presented here.

Electrons, at surface density  $n$ , are constrained to move in the  $X$ - $Y$  plane defined by the liquid-vapor interface of helium situated between electrodes of diameter 20 mm at  $z = h$  and  $z = -d$  ( $d + h = 1.95 \pm 0.05$  mm).  $V_c = 2e^2(\pi n)^{1/2}/(1 + \epsilon)$  is a measure of the Coulomb electron-electron interaction screened by the dielectric constant  $\epsilon$  of the helium substrate. For the density range of these experiments,  $n \approx 10^9$  cm<sup>-2</sup>, the system is classical and should be well characterized by the single dimensionless variable  $\Gamma = V_c/T$ . Two immediate consequences of this are that phases are delimited by  $\Gamma = \text{const}$  and that the shear modulus has the form

$$\mu = \mu_0 f(\Gamma), \text{ with } f(\infty) = 1 \text{ and } f(0) = 0, \quad (1)$$

$\mu_0 = \gamma_0 V_c / a_0^2$  being the zero-temperature value,  $a_0$  the lattice constant, and  $\gamma_0 = 0.160$ .<sup>4</sup>  $\mu \neq 0$  signifies elastic response to shear; for a liquid,  $\mu \rightarrow 0$  for  $\omega \rightarrow 0$ . Static measurements of  $\mu$  would be ideal, but experimentally difficult, and so we measure  $\mu$  by looking for its effects on a transverse coupled mode of the electrons and the ripples.

The vibrational spectrum is shown in Fig. 1. On a flat undeformable substrate, the longitudinal

( $l$ ) and transverse ( $t$ ) branches have the form shown in the inset. For  $k \ll n^{1/2}$

$$\begin{aligned} \omega_l^2(\vec{k}) &= 4\pi e^2 n k / m (\coth kh + \coth kd), \\ \omega_t^2(\vec{k}) &= \mu k^2 / mn. \end{aligned} \quad (2)$$

But when the substrate is deformable the low-wave-vector limit is altered.<sup>5</sup> An electric field<sup>6</sup>  $E$  pushes the electron lattice against the liquid surface which in its turn takes on a nonzero time-averaged deformation. The surface profile becomes a lattice of dimples, one for each electron

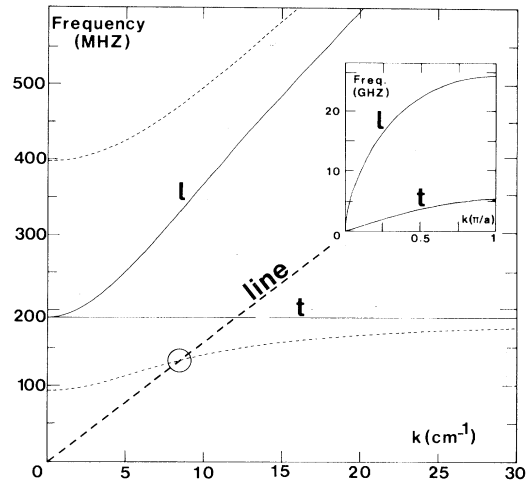


FIG. 1. Vibrational spectrum for two-dimensional electron solid. The inset shows the entire Brillouin zone; the principal figure, the small- $k$  region. The parameters are those of one of our experiments:  $n = 5.8 \times 10^8$  cm<sup>-2</sup>,  $h = 275$   $\mu$ m,  $T = 425$  mK. For magnetic field  $H = 0$ , the longitudinal ( $l$ ) and transverse ( $t$ ) "optical" branches (solid curves) meet for  $k = 0$  at the finite frequency  $\omega_0$  of Eq. (4). A finite magnetic field mixes these two branches to give the light-dashed curves ( $H = 110$  G). The heavy-dashed line is the dispersion of the electromagnetic coupling structure. The modes which couple only lightly to the electromagnetic field are not shown.

site and typically about  $\frac{1}{10}$  Å deep. The horizontal motions of the two lattices are coupled via the force pushing the electrons into their dimples. An approximate description of the dynamics may be based on a Fourier analysis around the reciprocal-lattice vectors  $\{g\}$ ; if this series is broken up into sets of  $N_g$  terms for each  $|\vec{g}| = g$ , the translation of each such group can be described by a two-dimensional position vector  $\vec{u}_g$  whose dynamic response is inertial with effective mass per site of  $M_g = (|eE|^2 \bar{n}_g^2 / 2m) N_g / \alpha \Omega_g^2$ . In this expression,  $\bar{n}_g$  is a time average of the Fourier component  $g$  of the density,  $\alpha$  is the surface tension, and  $\Omega_g^2 = (\alpha/\rho) g^3$  is the frequency of the corresponding capillary-wave mode if  $\rho$  is the density of the liquid set in motion. The coupling between  $\vec{u}_g$  and the electron position  $\vec{u}$  by the trapping potential  $\frac{1}{2} M_g \Omega_g^2 |\vec{u} - \vec{u}_g|^2$  leads to a set of eigenvalue equations,<sup>6</sup> which, upon introduction of the coupling between longitudinal and transverse motions by a normal magnetic field, become<sup>7</sup>

$$D_l(\vec{k}) D_t(\vec{k}) = \omega_c^2 \omega_c^2, \quad (3)$$

$$D_p(\vec{k}) = \omega_p^2(\vec{k}) - \omega^2 \left( 1 + \sum_g \frac{M_g}{m} \frac{\Omega_g^2}{\Omega_g^2 - \omega^2} \right); \quad p = l, t,$$

where  $\omega_c = eH/mc$  is the cyclotron frequency.

For our experiments, the coupling is strong ( $M_{g_0} \gg m$ ) and the overwhelming part of the electronic motion is found in the antiphase "optical" modes whose frequencies

$$\omega_p^2(\text{opt}, \vec{k}) \approx \omega_0^2 + \omega_p^2(\vec{k}),$$

$$\omega_0^2 \approx (M_{g_0}/m) \Omega_{g_0}^2, \quad (4)$$

are shown in Fig. 1. For clarity we have not shown the others, of which the longitudinal in-phase "acoustic" mode and two capillary-wave-like modes were first observed by Grimes and Adams,<sup>1</sup> demonstrating the existence of the solid phase; they too reflect the fluctuations and can in principle be used in the same way, but are more subject to uncertainties in  $k$ . The  $\omega_0^2 \approx (e^2 E^2 / 2\alpha mn) \sum N_g n_g^{-2}$  is reduced by thermal fluctuations in the electron density in much the same way as are Bragg peak intensities and to measure it leads to the fluctuation intensity  $T/\mu$ . Because the transverse optical branch is flat for  $\omega_t(\vec{k}) \ll \omega_0$  we measure its  $k \rightarrow 0$  frequency to determine  $\omega_0$ .

Our experiment was designed to measure  $\omega_t(\text{opt}, \vec{k})$  in the two limits  $k \lesssim 20 \text{ cm}^{-1}$  and  $k \approx 500 \text{ cm}^{-1}$ . We report here our results for the low- $k$  region. The interaction with the system is as-

sured by the electromagnetic field configuration [see formula (5)] set up by a meander transmission line on the lower electrode which transmits the radio frequency power from a swept-frequency (1–400 MHz) source to a detector. The lower electrode constitutes the ground plane for the 240- $\mu\text{m}$  full-wavelength meander conductor etched onto a  $20 \times 20 \text{ mm}$  portion of a 5- $\mu\text{m}$ -copper, 25- $\mu\text{m}$ -Kapton sandwich. The output from this line is amplified by a low-noise broad-band amplifier before being detected by a balanced mixer whose reference is derived from a parallel arm of equal phase delay. To separate that part of the response due to the electrons, this output is further analyzed by a low-frequency ( $\sim 1 \text{ kHz}$ ) phase-sensitive detector synchronized with a modulating potential applied across the cell.  $T$  is measured to  $\pm 5 \text{ mK}$  by carbon resistance thermometry,  $d$  to  $\pm 20 \mu\text{m}$  by interelectrode capacitance, and  $n$  to  $\pm 5\%$  by current integration, use of Gauss's theorem, and/or capillary-wave frequencies. The horizontal electric field of the meander line, averaged over its width, is given approximately by

$$\vec{E} = \hat{x} \sum E_s \sinh[k_s(h-z)] \exp[i(k_s x - \omega t)], \quad (5)$$

$$k_s = \omega/v + s k_L, \quad s = 0, \pm 1, \dots,$$

where  $k_L \approx 520 \text{ cm}^{-1}$ ,  $v \approx 10^8 \text{ cm sec}^{-1}$ , and  $E_s \approx (Z_0 P_{\text{in}})^{1/2} k_s / \sinh[k_s(d+h)]$  with  $Z_0 \approx 50 \Omega$  and  $P_{\text{in}} \approx 10 \text{ nW}$ . The  $s=0$  branch is superposed on Fig. 1; in the presence of coupling there will be a resonant reaction on the line whenever it crosses an electron branch. The field being longitudinal, the coupling to the transverse branch is effected by the Lorentz force in the applied magnetic field.<sup>8</sup>

The experimental curves of Fig. 2 show how the well-defined low-temperature resonance moves to lower frequency with increasing temperature. It approaches a limit of finite frequency at which the signal loses a factor of 5 in intensity over a relative temperature interval of 1% (700 to 707 mK); the longitudinal acoustic mode, not visible on the scale of the figure, is observed to disappear simultaneously. On re-cooling there is no sign of hysteresis. The absorption maxima (zero crossings of the phase detected signal) are identified with the intersection encircled in Fig. 1. By putting this couplet ( $\omega, k = \omega/v$ ) into Eq. (3) we deduce directly the sum term therein.

To extract the elastic moduli from experimental data, we must relate them to the time average  $\bar{n}_g$

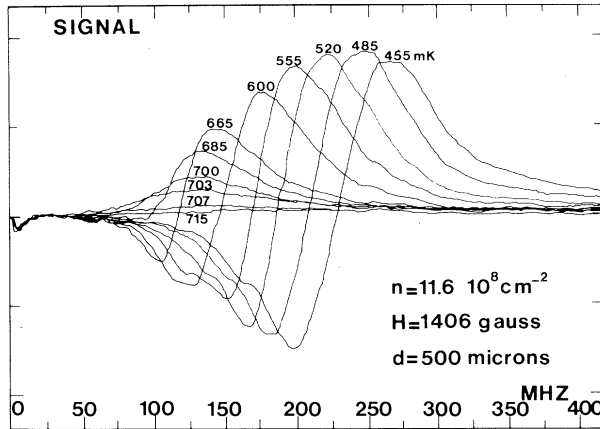


FIG. 2. A set of the observed signals from a given sample for a series of temperatures. At 715 mK, the liquid phase exhibits no transverse mode. When the electrons solidify at  $T_m \approx 707$  mK, the transverse mode appears at finite frequency over less than 5 mK.

occurring in the electron-surface coupling. The central problem here is what time average; because the deformation described by a given  $g$  can only respond on a time scale longer than  $\Omega_g^{-1}$ , it averages over any faster motion of the electrons. This average differs from that giving rise to the usual Debye-Waller factor<sup>9</sup> by the presence of this low-frequency cutoff to give

$$\bar{n}_g \approx n \exp(-\frac{1}{4} g^2 \bar{u}^2) \approx n \exp(-\frac{1}{2} \eta_g) \ln(\omega_D / \Omega_g), \quad (6)$$

where the last expression is only valid for classical statistics and a linear dispersion relation.<sup>10</sup> This introduces the critical-type index  $\eta_g = g^2 T / 4\pi \mu'$ , where  $\mu' = \mu / (1 + \delta/2)$ . We have written the Poisson ratio  $\sigma = 1 - \delta$  because we expect  $\delta \ll 1$  for this nearly incompressible Coulomb system. The presence of defects near  $T_m$  is estimated<sup>11</sup> to give  $\delta \approx 0.08$ . Solving for  $\eta_g$  and hence for  $\mu' a_0^2$  (taken to be independent of  $k$  and  $\omega$ ), we obtain the values reported in Fig. 3. In particular, at the melting temperature  $T_m$  we find that

$$\mu'(T_m^-) a_0^2 / T_m = 4\pi(1.1 \pm 0.1) \quad (7)$$

for all the samples measured. For comparison the Kosterlitz-Thouless criterion<sup>12,13</sup> deduced from the model of melting in two dimensions by dissociation of dislocation pairs gives

$$\mu'(T_m^-) a_0^2 / T_m = 4\pi / (1 - \delta^2/4). \quad (8)$$

As for  $\mu/\mu_0$ ,  $\mu'/\mu_0$  as a function of  $1/\Gamma$  should give the same curve  $f(\Gamma)$  for the three samples. The deviation from scaling of Fig. 3 may be partly explained by a bad choice of  $\omega_{\min}$ , although a

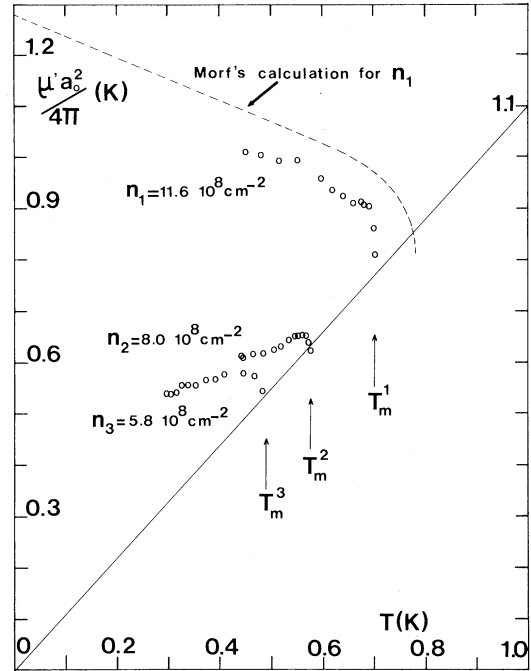


FIG. 3. Elastic modulus  $\mu'$  deduced from the experimental data for three samples.  $\mu' a_0^2 = \mu a_0^2 / (1 + \delta/2)$  is plotted vs temperature;  $\delta$  is the deviation of Poisson ratio from 1 and  $\mu$  is the shear modulus. The straight line is the fit  $\mu' a_0^2 / T = 4\pi(1.1)$  to  $\mu'(T_m^-)$ . The magnetic fields were  $H = 1400, 340, \text{ and } 110$  G for  $n_1 = 11.6 \times 10^8 \text{ cm}^{-2}$ ,  $n_2 = 8.0 \times 10^8 \text{ cm}^{-2}$ , and  $n_3 = 5.8 \times 10^8 \text{ cm}^{-2}$ , respectively. The result of Morf's (Ref. 11) molecular dynamics calculation for  $\mu(\Gamma)$  has been transcribed for the density  $n_1$ .

variation of  $\omega_{\min}$  by 50% only changes  $\mu'(T)$  by 10% near  $T_m$ . The results of Morf's<sup>11</sup> molecular dynamics calculation of  $\mu$  have been transcribed on the figure for comparison.

Some comments: (i) The phase boundary is well characterized by a sample-independent value of  $\Gamma = 140 \pm 10$ . (ii) We have no evidence for or against a third (e.g., hexatic<sup>13</sup>) phase. (iii) The existence of shear elasticity for  $T < T_m$  and  $\omega > \Omega_{g_0}$  is demonstrated by the nondivergence of the fluctuations. (iv) The amplitude of  $\mu(T_m^-)$  scales as expected from (1). Its value lends support to the Kosterlitz-Thouless melting mechanism as does, in a less quantitative manner, the observed form near  $T_m$ . We do not know how to evaluate the error introduced by the hypothesis of frequency independence of  $\mu$ , but we have tried to estimate that due to a wave-vector dependence of the type<sup>13</sup>  $\mu(k; T_m^-) = \mu(0, T_m^-)(1 + \text{const}/\ln ka)$ : Evaluating the constant very roughly by supposing that  $\mu$  for  $\ln ka = 1$  is given by a linear extrapolation

tion from the low-temperature region, we estimate that  $\mu(\text{expt}) - \mu(k=0) \approx 0.1 \mu\text{m}$ . We hope to have more detailed and precise information on  $\mu(k, T)$  from the direct measurement of  $c_i$  at the large meander-line wave vector  $k_L$ .

We take pleasure in thanking our colleagues, particularly Jacqueline Poitrenaud and Didier Marty. A. Valdès gratefully acknowledges the financial aid of a bursary from the French External Affairs Ministry.

<sup>1</sup>C. C. Grimes and G. Adams, Phys. Rev. Lett. **42**, 795 (1979).

<sup>2</sup>A. S. Rybalko, B. N. Esel'son, and Yu Z. Kovdrya, Fiz. Nizk. Temp. **5**, 947 (1979) [Sov. J. Low Temp. Phys. **5**, 450 (1979)].

<sup>3</sup>D. Marty, J. Poitrenaud, and F. I. B. Williams, J. Phys. (Paris) Lett. **41**, L311 (1980).

<sup>4</sup>L. Bonsall and A. A. Maradudin, Phys. Rev. B **15**, 1959 (1977). The hypothesis of a triangular lattice is supported by the progression of the ripple mode frequencies (Ref. 1).

<sup>5</sup>D. S. Fisher, B. I. Halperin, and P. M. Platzman,

Phys. Rev. Lett. **42**, 798 (1979).

<sup>6</sup>A polarization term  $(\epsilon - 1)ek^2 \ln(\beta/k)/8(\epsilon + 1)$  should be added to  $E$ , but it is usually small ( $\beta^{-1} = 41 \text{ \AA}$ ).

<sup>7</sup>F. Gallet, third cycle thesis, University of Paris, 1980 (unpublished). {D. S. Fisher and V. B. Shikin, Pis'ma Zh. Eksp. Teor. Fiz. **31**, 228 (1980) [JETP Lett. **31**, 208 (1980)], give the  $k=0$  limit.}

<sup>8</sup>G. Deville, F. Gallet, D. Marty, J. Poitrenaud, A. Valdès, and F. I. B. Williams, in *Ordering in Two Dimensions*, edited by S. K. Sinha (North-Holland, New York, 1981).

<sup>9</sup>Y. Imry and L. Gunther, Phys. Rev. B **3**, 3939 (1971).

<sup>10</sup>We use quantum statistics when necessary ( $\omega \gtrsim T$ ). Furthermore, when  $\omega_0 > \Omega_g$ , the gap in the modified excitation spectrum leads to a self-consistent approach where  $\bar{u}^2 = \int d^2k \bar{u}_{\vec{k}}^{-2}$  is summed over the whole of the "optical" branches. The magnetic fields used have negligible effect on this sum, even when quantum effects are accounted for, as long as the frequency of the lower optical branch remains higher than  $\Omega_g$ .

<sup>11</sup>R. Morf, Phys. Rev. Lett. **43**, 931 (1979).

<sup>12</sup>J. M. Kosterlitz and D. J. Thouless, J. Phys. C **6**, 1181 (1973).

<sup>13</sup>D. R. Nelson and B. I. Halperin, Phys. Rev. B **19**, 2457 (1979).

## Radiation from Two-Dimensional "Molecular" Bound States of Electrons Channeled in Diamond

J. U. Andersen, S. Datz,<sup>(a)</sup> E. Lægsgaard, J. P. F. Sellschop,<sup>(b)</sup> and A. H. Sørensen  
*Institute of Physics, University of Aarhus, DK-8000 Aarhus C, Denmark*

(Received 26 February 1982)

Axially channeled electrons are captured into bound states of the "atomic-string" potential. When two rows lie in close proximity as in the  $\langle 110 \rangle$  direction of diamond, the potentials overlap, forming a saddle point between the rows. For 4-MeV electrons in the  $\langle 110 \rangle$  diamond potential, the  $2p$  level lies above the saddle point, and molecular states are formed. The observation of radiation arising from transitions of these states is reported. Spectral information is used to deduce electron-density enhancement in the C-C bond.

PACS numbers: 61.80.Mk, 41.70.+t

For axial channeling of electrons at a few megaelectronvolts in low- $Z$  materials, transitions between bound states of transverse motion<sup>1</sup> give rise to a line spectrum of "channeling radiation" at energies of a few kiloelectronvolts in the forward (beam) direction.<sup>2,3</sup> In the diamond lattice, the atomic strings along the  $\langle 110 \rangle$  direction are arranged in pairs, and the bound states of transverse motion have molecular character. In analogy with a diatomic molecule, they may be classified as bonding and antibonding orbitals, and the splitting between these states, which may be derived from the radiation spectra, is

particularly sensitive to charge accumulation in the tetrahedral bonds between carbon atoms. The results represent the first clear evidence from channeling radiation of deviations in a crystal from the electron density obtained from overlapping atomic densities. In contrast, for previous experiments on silicon, calculations with atomic scattering factors derived from relativistic Hartree Fock calculations were found to reproduce the measured line energies for channeling radiation within the experimental uncertainty.<sup>3,4</sup>

An electron beam from the 5-MV Van de Graaff